USCAP

ARTICLE

Check for updates

Long noncoding RNA MIR22HG promotes Leydig cell apoptosis by acting as a competing endogenous RNA for microRNA-125a-5p that targets N-Myc downstream-regulated gene 2 in late-onset hypogonadism

Yan-ling Liu[1], Feng-jiao Huang[1], Pei-jie Du[1], Jiao Wang[1], Feng Guo[1], Ming-wei Shao[1], Yi Song[1], Yan-xia Liu[1] and Gui-jun Qin[1]✉

Leydig cells (LCs) apoptosis is responsible for the deficiency of serum testosterone in Late-onset hypogonadism (LOH), while its specific mechanism is still unknown. This study focuses on the role of long noncoding RNA (lncRNA) MIR22HG in LC apoptosis and aims to elaborate its regulatory mechanism. MIR22HG was up-regulated in the testicular tissues of mice with LOH and H_2O_2-treated TM3 cells (mouse Leydig cell line). Interference of MIR22HG ameliorated cell apoptosis and upregulated miR-125a-5p expression in H_2O_2-treated TM3 cells. Then, the interaction between MIR22HG and miR-125a-5p was confirmed with RIP and RNA pull-down assay. Further study showed that miR-125a-5p downregulated N-Myc downstream-regulated gene 2 (NDRG2) expression by targeting its 3′-UTR of mRNA. What's more, MIR22HG overexpression aggravated cell apoptosis and reduced testosterone production in TM3 cells via miR-125a-5p/NDRG2 pathway. MIR22HG knockdown elevated testosterone levels in LOH mice. In conclusion, MIR22HG up-regulated NDRG2 expression through targeting miR-125a-5p, thus promoting LC apoptosis in LOH.

Laboratory Investigation (2021) 101:1484–1493; https://doi.org/10.1038/s41374-021-00645-y

INTRODUCTION

Late-onset hypogonadism (LOH) is a clinical and biochemical syndrome that is widespread among middle-aged and older men. LOH is characterized by reduced serum testosterone levels and clinical symptoms that are associated with advancing age[1]. The core pathogenesis of LOH is a deficiency in serum testosterone, which is mainly produced by the Leydig cells (LCs) in the testis[2]. It has been proven that the excessive apoptosis of LCs leads to a reduction in serum testosterone, thus exacerbating LOH development[3]. Thus, clarifying the mechanism of LC apoptosis is beneficial in that it can provide a more in-depth understanding of the pathogenesis of LOH.

N-Myc downstream-regulated gene 2 (NDRG2) is a member of NDRG family and plays a role in the regulation of cell proliferation[4], differentiation[5], and apoptosis[6]. A previous study found that NDRG2 modulated testicular development and spermatogenesis in rats[7], and its expression boosted the apoptosis of germ cells in a cryptorchidism rat model[8]. Recent evidence has shown that NDRG2 regulated by NF-κB is essential for the apoptosis of LCs in both human and murine infertile testes[9], validating NDRG2 as a positive regulator for LC apoptosis.

MicroRNA (miRNA)-125a-5p is well known as a tumor suppressor gene in various types of cancer[10,11]. Recently, growing evidence has indicated that miR-125a-5p is also related to the development of LOH. Chen et al.[12] found that miR-125a-5p was down-regulated in the plasma of LOH patients. Moreover, the modulatory effect of miR-125a-5p on cell apoptosis has also been discussed[13]. Furthermore, bioinformatics analysis has predicted that there is a complementary binding site between miR-125a-5p and NDRG2, implying that miR-125a-5p may regulate the apoptosis of LCs in the development of LOH by binding to NDRG2.

Several long non-coding RNAs (lncRNAs) have been identified as testis germ cell-specific lncRNAs and play key roles in testicular development and spermatogenesis[14,15]. While the specific effect of lncRNAs on the apoptosis of LCs and pathogenesis of LOH is not yet clear. It has been reported that the high expression of anti-apoptotic protein B-cell lymphoma-2 (Bcl-2) restrains LCs from apoptosis[2]. LncRNA MIR22HG has been shown to suppress Bcl-2 expression via targeting human antigen R[16], implying that MIR22HG may participate in the regulation of LC apoptosis. In our preliminary study, a clear elevation of MIR22HG expression was noted during the apoptosis of mouse LC cell line TM3, and potential binding sites between MIR22HG and miR-125a-5p were forecast by LncBase Predicted v.2. Moreover, increasing evidence has confirmed that lncRNAs can function as competing endogenous RNAs (ceRNAs), binding to miRNA and removing their suppressive effect on mRNA expression[17]. Above all, we hypothesized that MIR22HG could act as a ceRNA to elevate NDRG2

[1]Department of Endocrinology and Metabolism, The First Affiliated Hospital of Zhengzhou University, Zhengzhou, PR China. ✉email: hyqingj@zzu.edu.cn

Received: 29 January 2021 Revised: 12 July 2021 Accepted: 14 July 2021
Published online: 26 August 2021

expression by targeting miR-125a-5p, thus aggravating LC apoptosis in LOH.

MATERIALS AND METHODS

Cell culture

Mouse LC line TM3 was purchased from the American Type Culture Collection (USA), maintained in Dulbecco's modified Eagle's medium-Ham's F12 medium mixture (1:1) containing 2.5% fetal bovine serum and 5% horse serum, and cultured with 5% CO_2 at 37 °C. The TM3 cells were then incubated with H_2O_2 at different concentrations (100, 200, and 400 μM), and after 8 h, the cells were harvested for the following experiments.

Cell transfection

The TM3 cells were cultured in 6-well plates with a concentration of 4×10^5 cells/well. When the cells were cultured to 70% confluence, they were transfected with RNAi-vector (si-MIR22HG), overexpression vectors (pcDNA-MIR22HG, miR-125a-5p mimic), or relative negative controls (si-NC, pc-DNA, mimic-NC) using Lipofectamine 2000 (Invitrogen, USA).

Quantification of apoptosis

The TM3 cells were seeded in 6-well plates at 4×10^5 cells/well and treated with 100, 200, or 400 μM of H_2O_2. After 8 h, the cells were harvested and apoptosis was measured utilizing the Annexin V-FITC Apoptosis Detection Kit (Shanghai Yeasen Biotechnology Co., Ltd. China). In brief, the TM3 cells were reacted in order with 5 μl Annexin V-FITC and 5 μl Propidium Iodide Staining Solution in the dark. A flow cytometer (Beckman Coulter) was used to examine cell apoptosis.

Cell proliferation assay

A BeyoClick™ EdU Cell Proliferation Kit (Beyotime, China) was employed to assay TM3 cell proliferation. A total of 10 μM EdU was added into each well and reacted with the TM3 cells for 3 h. A 500 μl click reaction buffer containing $CuSO_4$ and Alexa Fluor 488 was then added to each well. After being ounterstained with DAPI, the cells were immediately imaged by IXplore microscopy (Olympus Corporation, Japan).

Quantitative RT-PCR

Total RNA samples were extracted from the TM3 cells or the testis tissues of LOH mice using TRIzol Reagent (TW-reagent, China). After inverse transcription into cDNA, the expression levels of MIR22HG, miR-125a-5p, and NDRG2 in the samples were analyzed utilizing a SYBR Green PCR kit (QIAGEN, Germany) with an ABI 7500 real-time PCR system (Applied Biosystems, USA). The amplification profile was denatured at 95 °C for 10 min, followed by 45 cycles of denaturation at 95 °C for 15 s, annealing at 60 °C for 30 s, and extension at 72 °C for 1 min.

U6 is a type of small nuclear RNA (snRNA) that is highly conserved among species. U6 snRNA located at the heart of a spliceosome participates in the processing of mRNA precursors, and it is very stable, with a half-life value of ~24 h[18]. Hence, U6 was used to normalize the relative expression of miR-125a-5p, and β-actin was used to normalize the relative expression of MIR22HG and NDRG2. The progression of normalization was as follows: the quantification data were expressed as cycle threshold (Ct). The Ct values were averaged for three duplicates. The averaged Ct was normalized as a difference in Ct values (ΔCt) between each sample and the U6/β-actin gene. The ΔCt values were normalized with respect to the ΔCt values of the control (ΔΔCt). The relative gene expression was reported as a fold change ($2^{-\Delta\Delta Ct}$).

The primers used in this study are shown in Table 1.

Western blot

The protein levels of NDRG2, cleaved caspase-3, Bax, and Bcl-2 in the TM3 cells and testis tissues of LOH mice were detected by western blot. After being isolated from the TM3 cell lysate or testis tissues of LOH mice using RIPA (Shanghai Absin Biological Technology Co., Ltd., China), the protein samples were subjected to 10% sodium dodecyl sulfate-polyacrylamide gel electrophoresis and then transferred to a PVDF membrane (ThermoFisher Scientific, USA). The membranes were then reacted with blocking buffer, primary antibodies, and secondary antibodies. The IBright FL1500 Intelligent Imaging System (ThermoFisher, USA) was used to visualize the membranes. The primary antibodies used in this study were as follows: anti-NDRG2 antibody (ab174850, Abcam, UK), anti-Bax antibody (ab182733, Abcam), anti-Bcl-2 antibody (sc-7382, Satra Cruz Biotechnology, USA), and anti-cleaved caspase-3 (9664T, Cell Signaling Technology, USA).

ELISA assay

The levels of testosterone in the TM3 cells or the serum and testes of the LOH mice were analyzed by ELISA based on the instructions of a Testosterone ELISA kit (Biovision, USA). The concentration of testosterone was presented as ng per 10^5 cells in the TM3 cells, ng per ml in the serum of the LOH mice, and ng per g in the testes of the LOH mice. The sensitivity of the ELISA assay was 10 pg/tube, with intra-assay and inter-assay coefficients of variation of 11.2% and 9.6%, respectively.

Dual-luciferase reporter gene assay

To verify the combination of miR-125a-5p and the 3′UTR region of NDRG2, NDRG2-3′-UTR-wild type (WT NDRG2), and NDRG2-3′-UTR-mutant (MUT NDRG2) were each synthesized and inserted into pmirGLO plasmids, respectively. 293T cells received a co-transfection of the 0.5 μg plasmid (WT NDRG2 or MUT NDRG2) and 20 nM miR-125a-5p mimic or mimic-NC. After 2 days, the cells were lysed and the activities of luciferase were measured with a Dual-Luciferase Reporter Assay Kit (Promega, China).

RNA immunoprecipitation (RIP)

A total of 1.3×10^7 TM3 cells were collected and lysed. Protein A/G magnetic beads bound with AGO2 antibody (MA5-23515, Thermo Fisher) or mouse IgG (ab6789, Abcam) were added into the TM3 cell lysate. The proteins in the immunoprecipitate of the AGO2 or IgG were removed using Proteinase K. The RNA samples were then purified from the immunoprecipitate of the AGO2 or IgG and used to detect the expression of MIR22HG and miR-125a-5p by qRT-PCR.

RNA pull-down assay

Biotin RNA Labeling Mix (Roche, Switzerland) was employed to obtain the biotin (Bio)-labeled miR-125a-5p wild-type (wt). The TM3 cells were harvested and lysed, followed by reaction with Bio-miR-125a-5p wt and magnetic beads. The MIR22HG level in the compound pulled down by Bio-miR-125a-5p-wt was measured by qRT-PCR. Bio-miR-125a-5p-wild-mutant (mut) served as a negative control.

Table 1. The sequences of primers used in this study were shown as below.

Genes	Forward primer (5′–3′)	Reverse primer (5′–3′)
β-actin	ACTGCCGCATCCTCTTCCT	TCAACGTCACACTTCATGATGGA
MIR22HG	CCAGTTGAAGAACTGTTGCCC	CGTATCATCCACCCTGCTGT
NDRG2	TCGTGCGGGTTCATGTGGATGC	TGTGTCCGGGTGGTTCAGAGCA
U6	CGCTTCACGAATTTGCGTGTCAT	CGCTTCACGAATTTGCGTGTCAT
miR-125a-5p	TCCCTGAGACCCTTTAACCTGTGA	
hsa-miR-361-5p	TTATCAGAATCTCCAGGGGTAC	
hsa-miR-150-5p	TCTCCCAACCCTTGTACCAGTG	
hsa-miR-133a-3p	TTTGGTCCCCTTCAACCAGCTG	
hsa-miR-1301-3p	TTGCAGCTGCCTGGGAGTGACTTC	

The Bio-labeled MIR22HG probe was obtained as above, and the miR-125a-5p level in the complex that was pulled down by the MIR22HG probe was detected by Northern blot analysis as described previously[19].

Mouse model of LOH

Laboratory Animal Resources, Chinese Academy of Sciences (Beijing, China) provided the male C57BL/6 mice (24 or 2 months old) used in this study. The serum testosterone of each mouse was quantified by using the blood collected from the retrobulbar space, and sexual behavior assays were conducted as previously reported[20].

Six of the older male mice with LOH symptoms (hyposexuality, decreased morning erections, decreased energy, etc.) and a serum testosterone concentration below 8 ng/ml were adopted into the LOH group, and another six young adult male mice were adopted into the control group. A tail suspension test was performd on each mouse and blood was collected from the retrobulbar space. The mice were then euthanized, and the testicular tissues were collected.

To evaluate the effect of MIR22HG on LOH, the older male mice with LOH symptoms and a serum testosterone concentration below 8 ng/ml were employed ($n = 18$) and randomly divided into three groups ($n = 6$ in each group): LOH, LOH + lentivirus vectors containing shRNA-MIR22HG (Lenti-sh-MIR22HG), and LOH + the negative control of Lenti-sh-MIR22HG (Lenti-shRNA). Lenti-sh-MIR22HG and Lenti-shRNA were synthesized by Ribobio (China). The mice were anesthetized with Nembutal. In the LOH +Lenti-sh-MIR22HG group ($n = 6$), Lenti-sh-MIR22HG (30 μl, 1×10^8 IU/ml) was injected into the testis. In the LOH +Lenti-shRNA group ($n = 6$), Lenti-shRNA-control (30 μl, 1×10^8 IU/ml) was injected in the same position. In the LOH group ($n = 6$), the mice received same volume of saline in the same position. Serum samples of each group were collected from tails 1 day before and 7, 14, 21, and 28 days after injection to quantify serum testosterone. A tail suspension test was performed 1 day before and 28 days after injection. The mice were euthanized at 28 days after injection, and testicular tissues were collected. All protocols in this study were approved by the Ethics Committee of the First Affiliated Hospital of Zhengzhou University.

Histological assessment

Testicular tissues collected from mice were prepared into 4 μm-thick sections for hematoxylin–eosin (H&E) staining. The H&E staining was conducted using an H&E staining kit purchased from Boster Biological Technology CO., Ltd (China).

Tail suspension test

We performed the tail suspension test as previously described previously[21]. In brief, the mice were suspended individually by the tail to a hook connected to a strain gauge using packaging tape (placed 2 cm from the tip of the tail). The detection lasted for 6 min and an automated system was used to measure the duration of immobility.

Statistical analysis

The experimental results were expressed as mean ± standard deviation (SD) and analyzed using GraphPad 7.0 Prism. The differences were analyzed with a Student's *t* test or one-way analysis of variance with the Newman–Keuls post hoc test. The results were considered statistically significant when $P < 0.05$.

For the entire in vitro study, each sample included three biological replications that were measured in one technique replications. For the in vivo study, three sections per group were used for the HE staining and six samples per group were used for the other experiments.

RESULTS

MIR22HG was up-regulated in the testicular tissues of mice with LOH

Six older male mice with LOH symptoms and a serum testosterone concentration below 8 ng/ml were adopted in the LOH group, and another six young adult male mice were adopted in the control group. As shown in Fig. 1a, the serum testosterone concentrations in the mice of the control group were significantly higher than that of mice of the LOH group. The results of the tail suspension test revealed more severe depressive symptoms in the mice of the LOH group relative to the mice of the control group (Fig. 1b). As compared to the mice of the control group, the LC numbers were reduced (Fig. 1c) and intratesticular testosterone concentrations (Fig. 1d) were apparently decreased in the mice of the LOH group. We then examined MIR22HG expression using qRT-PCR and found that MIR22HG was up-regulated in the testicular tissues of the mice in the LOH group as compared to the mice of the control group (Fig. 1e).

H_2O_2 treatment induced cell apoptosis and elevated MIR22HG expression in TM3 cells

During the process of cell metabolism, a large number of reactive oxygen species are produced, including H_2O_2. It has been proven that an accumulation of H_2O_2 can inhibit testosterone production in LCs and induce LC apoptosis in vitro[22]. Therefore, we used H_2O_2 at different concentrations (100, 200, and 400 μM) to stimulate the mouse LC cell line TM3. As shown in Fig. 2a, b, H_2O_2 induction promoted cell apoptosis and suppressed cell proliferation in the TM3 cells in a dose-dependent manner. In addition, with the aggravation of H_2O_2-induced apoptosis, testosterone production was decreased (Fig. 2c) and MIR22HG expression was increased, similarly, in a dose-dependent manner (Fig. 2d).

MIR22HG knockdown suppressed cell apoptosis and elevated miR-125a-5p expression in H_2O_2-treated TM3 cells

To define the role of MIR22HG in LC apoptosis, si-MIR22HG or si-control was transfected into TM3 cells. After transfection, the TM3 cells were then treated with 400 μm H_2O_2 for 8 h. The transfection efficiency of si-MIR22HG is shown in Fig. 3b, and the fluorescence images of si-MIR22HG transfection are shown in Fig. 3d. The apoptosis of the H_2O_2-stimulated TM3 cells was determined using a flow cytometer. The results showed that MIR22HG knockdown reduced the apoptosis of the TM3 cells induced by H_2O_2 (Fig. 3a). To explore the mechanism of MIR22HG aggravating cell apoptosis, several expression levels of miRNAs, which have been reported to be abnormally changed in the serum of LOH patients[12], were measured. The results showed that the H_2O_2 treatment increased miR-1301-3p expression, and decreased the expressions of miR-125a-5p, miR-361-5p, miR-150-5p, and miR-133a-3p. It's worth noting that MIR22HG interference only promoted miR-125a-5p mRNA level (Fig. 3c), indicating MIR22HG may induce LC apoptosis by targeting miR-125a-5p.

The interplay between MIR22HG, miR-125a-5p, and NDRG2 in TM3 cells

To evaluate the interplay between MIR22HG and miR-125a-5p, bioinformatics database LncBase Predicted v.2 was used to forecast their combination. The results showed there were potential binding sites between MIR22HG and miR-125a-5p (Fig. 4a). Next, RIP and RNA pull-down assays were conducted to determine the interplay between MIR22HG and miR-125a-5p in the TM3 cells. As shown in Fig. 4b, as compared with IgG, abundant MIR22HG and miR-125a-5p were detected in the immunocomplex of the AGO2 antibody. What is more, a great quantity of MIR22HG was detected in the complex pulled down by the Bio-miR-125a-5p-wt, and plenty of miR-125a-5p was accumulated in the complex pulled down by biotinylated MIR22HG probe (Fig. 4c). Furthermore, MIR22HG was overexpressed in the TM3 cells by pcDNA-MIR22HG transfection and the transfection efficiency is shown in Fig. 4d. A clear down-regulation of miR-125a-5p was observed in MIR22HG-overexpressed TM3 cells (Fig. 4e). These data determined that MIR22HG decreased miR-125a-5p expression via binding to it directly.

Using an online bioinformatics database (microRNA.org), we found that miR-125a-5p has putative binding sites with NDRG2 (Fig. 4f). To explore the effect of miR-125a-5p on NDRG2, Dual-Luciferase Reporter Assays were conducted. As compared to cells transfected

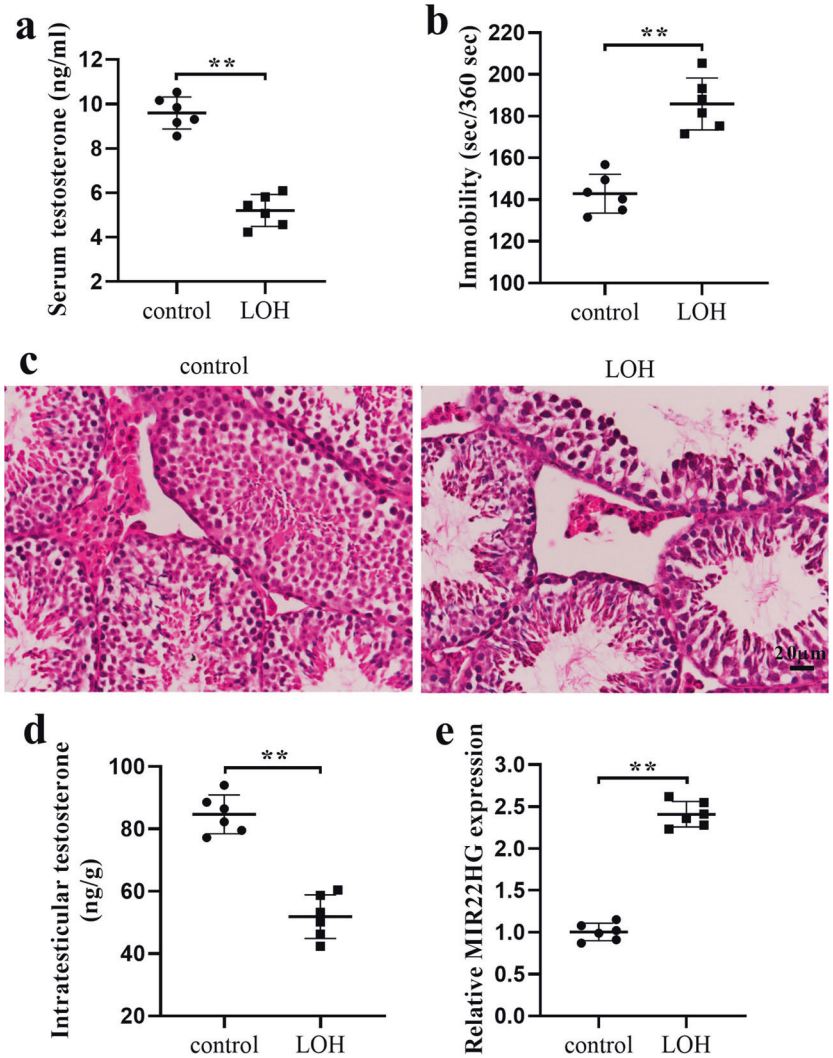

Fig. 1 MIR22HG was up-regulated in the testicular tissues of mice with late-onset hypogonadism (LOH). Six older male mice with LOH symptoms and a serum testosterone concentration below 8 ng/ml were adopted in the LOH group, and another six young adult male mice were adopted in the control group. **a** The serum testosterone concentration of mice in each group was measured by ELISA assay. **b** Tail suspension test. **c** Hematoxylin–eosin (H&E) staining was performed on the testicular tissues of mice in each group ($n = 3$ per group and the representative images were shown, scale bar = 20 μm). **d** Intratesticular testosterone concentration of mice in each group was measured by ELISA assay. **e** Relative MIR22HG expression in testicular tissues of mice in each group was measured using qRT-PCR. $^{**}P < 0.01$.

with mimic-NC, the luciferase activity of WT NDRG2 was significantly decreased in the cells transfected with miR-125a-5p-mimic (Fig. 4g), while neither miR-125a-5p-mimic nor mimic-NC had an effect on the activity of MUT NDRG2. Furthermore, miR-125a-5p was overexpressed in the TM3 cells by miR-125a-5p-mimic transfection, and the transfection efficiency is shown in Fig. 4h. The mRNA level and protein abundance of NDRG2 were all dramatically dropped in the miR-125a-5p-overexpressed TM3 cells (Fig. 4i, j). These data demonstrate that miR-125a-5p negatively regulated NDRG2 expression via binding to its 3′UTR.

Overexpression of miR-125a-5p reversed cell apoptosis and NDRG2 upregulation induced by pcDNA-MIR22HG in TM3 cells

To explore whether MIR22HG induced cell apoptosis by targeting miR-125a-5p, the following experiments were conducted. First, TM3 cells were transfected with pcDNA-MIR22HG, and this transfection overexpressed MIR22HG (Fig. 5d), repressed miR-125a-5p expression (Fig. 5e), increased NDRG2 mRNA level (Fig. 5f), enriched NDRG2 protein abundance (Fig. 5f), induced cell apoptosis (Fig. 5a), reduced cell proliferation (Fig. 5b), and resulted in a prominent reduction in testosterone concentration (Fig. 5c) in the TM3 cells. We then explored whether miR-125a-5p overexpression could partly reverse the effect of pcDNA-MIR22HG. As expected, the overexpression of miR-125a-5p with miR-125a-5p mimic partly reduced cell apoptosis (Fig. 5a), facilitated cell proliferation (Fig. 5b), and elevated testosterone concentrations (Fig. 5c) in the MIR22HG-overexpressed TM3 cells. Additionally, we also found that miR-125a-5p overexpression efficiently depressed the promotion of NDRG2 mRNA level and protein abundance induced by pcDNA-MIR22HG in the TM3 cells (Fig. 5f). These results show that MIR22HG promoted cell apoptosis in the TM3 cells via functioning as a ceRNA for miR-125a-5p to upregulate NDRG2.

MIR22HG knockdown promoted testosterone secretion in LOH mice

Next, to validate our in vitro findings further in vivo, Lenti-sh-MIR22HG/Lenti-shRNA (30 μl, 1×10^8 IU/ml) were injected into the testis of mice with LOH. The MIR22HG level, measured by qRT-PCR, confirmed that Lenti-sh-MIR22HG successfully silenced MIR22HG in the testis of the mice (Fig. 6e). H&E staining showed that as

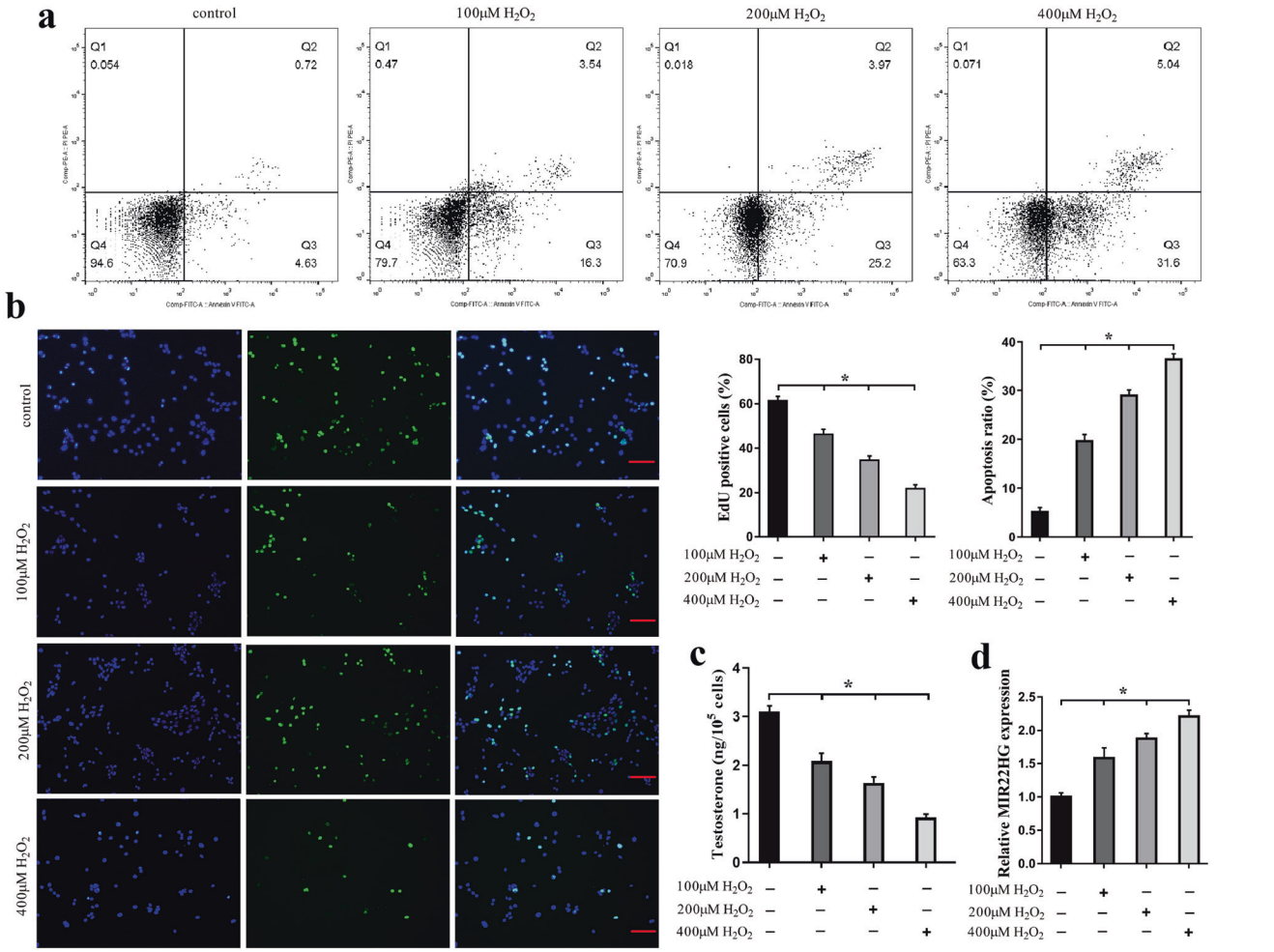

Fig. 2 H_2O_2 treatment induced cell apoptosis and up-regulated MIR22HG level in TM3 cells. Mouse LC cell line TM3 was incubated with different concentrations of H_2O_2 (100, 200, and 400 μM). **a** The ratio of apoptotic cells was quantified using flow cytometry. **b** Cell proliferation was detected using EdU immunofluorescence analysis (Scale bar = 100 μm) and the EdU positive cells (green) were calculated. DAPI (blue) was used to counterstain the cell nucleus. **c** The concentration of testosterone in cells was determined using ELISA. **d** The relative expression level of MIR22HG was determined using qRT-RCR. The cells without H_2O_2 treatment were used as control. *$P < 0.05$.

compared to mice in the group injected with Lenti-shRNA, the mice injected with Lenti-sh-MIR22HG exhibited more LCs and improved seminiferous tubule structure (Fig. 6a). As shown in Fig. 6b, d, MIR22HG knockdown elevated both serum and intratesticular testosterone concentrations. The results of the tail suspension test indicated that the MIR22HG knockdown effectively mitigated the depressive symptoms in the LOH mice (Fig. 6c). MIR22HG knockdown downregulated pro-apoptotic protein (cleaved caspase-3 and Bax) abundances and upregulated anti-apoptotic protein (Bcl-2) abundances (Fig. 6h). Furthermore, the miR-125a-5p level was increased (Fig. 6f) and NDRG2 was downregulated (Fig. 6g, h) in the Lenti-sh-MIR22HG-treated LOH mice, indicating that the miR-125a-5p/NDRG2 axis also took part in the therapeutic effect of MIR22HG knockdown in the LOH mice.

DISCUSSION

With the aggravating trend of an aging population, the number of men with LOH continuously increases. The etiology of LOH can be explained by several hypotheses, and among them, a deficiency in serum testosterone induced by LC apoptosis is considered a core mechanism[23]. This study identified a new regulatory pathway concerning LC apoptosis, that involves lncRNA MIR22HG, miR-125a-5p, and NDRG2. In brief, we clarified that a high expression of MIR22HG promoted LC apoptosis by upregulating NDRG2 via targeting miR-125a-5p, resulting in a deficiency of testosterone (Fig. 7). In the performance of this study, the significance of MIR22HG and miR-125a-5p in the pathogenesis of LOH was emphasized, providing novel perspectives on LOH progression and treatment.

Emerging evidence has shown that lncRNAs are closely related to testis development and spermatogenesis[24,25]. For example, Akhade et al. reported[26] that lncRNA mrhl RNA regulated the expression of genes pertaining to spermatogenesis via negatively regulating the Wnt pathway. Through microarray analysis, 1607 lncRNAs have been identified as testis-specific in mice[27], suggesting that lncRNAs participate in the development of male germ cells. To date, little is known about the role of lncRNAs in testosterone production and LC function. In this study, we found that MIR22HG level was notably elevated in the process of TM3 cell apoptosis. Furthermore, this study confirmed that a high expression of MIR22HG promoted LC apoptosis and decreased testosterone production both in vitro and in vivo. Our study enriches the understanding of the role of lncRNAs in the regulation of germ cells and reveals the promising role of MIR22HG as an effective target in LOH treatment.

The ceRNA hypothesis was proposed by Harvard researchers in 2011. This hypothesis states that various types of RNA (including lncRNA, circRNA, etc.) can completely bind to the same miRNA via base-pairing miRNA response elements, thus reducing the number of miRNAs available to target mRNAs and abolishing the

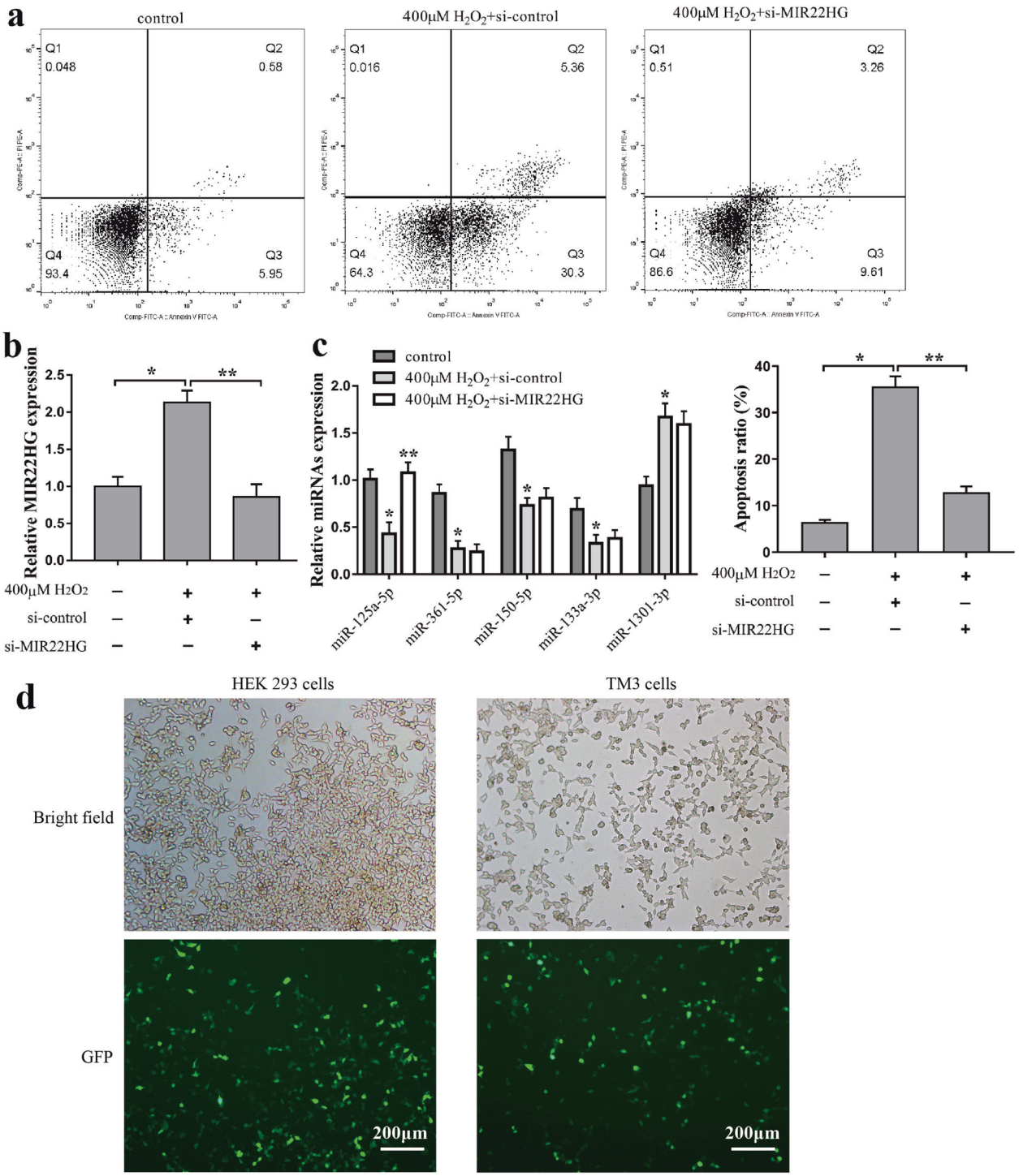

Fig. 3 MIR22HG aggravated cell apoptosis and down-regulated miR-125a-5p expression in TM3 cells. Si-MIR22HG or its negative control (si-control) was transfected into TM3 cells. Forty-eight hours after transfection, the TM3 cells were treated with 400 μM H_2O_2 for 8 h, and then the cells were harvested for the examination of (**a**) apoptosis ratio (*$P < 0.05$; **$P < 0.01$), **b** relative MIR22HG expression (*$P < 0.05$; **$P < 0.01$), and (**c**) relative expressions of miR-125a-5p, miR-361-5p, miR-150-5p, miR-133a-3p, and miR-1301-3p (*$P < 0.05$; **$P < 0.01$ vs. control). **d** Confocal laser scanning microscopic images of si-MIR22HG-transfected HEK 293 cells (left) and TM3 cells (right). The upper panels show the corresponding bright-field images of the cells. Scale bar = 200 μm.

downstream effects of these miRNAs on target mRNAs[17]. In hepatocellular carcinoma cells, MIR22HG adsorbed miR10Aa-5p and released nuclear receptor corepressor 2 expression, thus inhibiting cell proliferation[28], which confirmed the potential of MIR22HG to function as ceRNAs for miRNAs. In our study, in response to MIR22HG knockdown, cell apoptosis was decreased and miR-125a-5p expression was increased in H_2O_2-treated TM3 cells, indicting that MIR22HG may promote cell apoptosis via miR-125a-5p. The following RIP and RNA pull-down assay displayed there was a combination between MIR22HG and miR-125a-5p. Subsequently, NDRG2 was determined to be the target gene of miR-125a-5p and its expression was negatively regulated by miR-

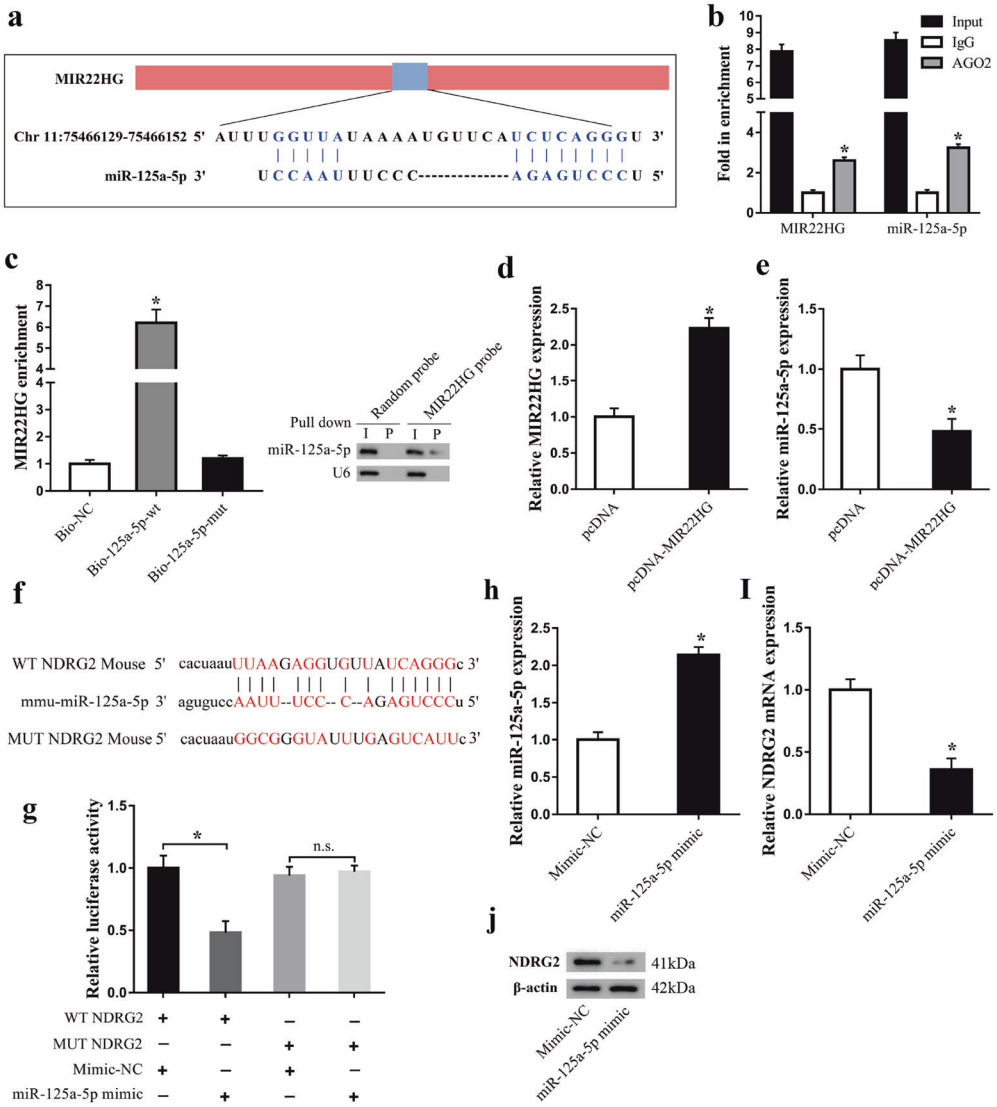

Fig. 4 The interplay between MIR22HG, miR-125a-5p, and N-Myc downstream-regulated gene 2 (NDRG2). a The potential binding sites between MIR22HG and miR-125a-5p forecasted by bioinformatics database (LncBase Predicted v.2). **b** RNA-binding protein immunoprecipitation (RIP) followed by qRT-PCR was performed to measure the endogenous combination of MIR22HG and miR-125a-5p. **c** Detection of MIR22HG using qRT-PCR in the samples pulled down by the biotinylated miR-125a-5p-wild type (Bio-miR-125a-5p-wt), biotinylated miR-125a-5p-mutation (Bio-miR-125a-5p-mut), and biotinylated negative control (Bio-NC) probe. Detection of miR-125a-5p using northern blot in the samples pulled down by the biotinylated MIR22HG probe and negative control (Random) probe. I input (10% samples were loaded); P pellet (100% samples were loaded). Then, TM3 cells were transfected with pcDNA-MIR22HG or pc-DNA, 48 h later, the cells were harvested and the expression levels of (**d**) MIR22HG and (**e**) miR-125a-5p were measured by qRT-PCR. **f** Putative binding sites between miR-125a-5p and NDRG2 were forecasted by Miranda. **g** Relative luciferase activities of NDRG2 wild type 3′-UTR (WT NDRG2) and NDRG2 mutant 3′-UTR (MUT NDRG2) in 293T cells transfected with miR-125a-5p mimic or negative control (Mimic-NC) were measured using the Dual-Luciferase Reporter Assay System (*$P < 0.05$). Then, TM3 cells were transfected with miR-125a-5p mimic or Mimic-NC, 48 h later, the cells were harvested for the examination of (**h**) miR-125a-5p expression and NDRG2 (**i**) mRNA and (**j**) protein levels. *$P < 0.05$ vs. IgG or Bio-NC or pcDNA or Mimic-NC.

125a-5p. These data confirm that MIR22HG released NDRG2 expression by functioning as the ceRNA for miR-125a-5p.

Previous studies of miR-125a-5p were focused on its effects on various malignancies such as gastric cancer[29], lung cancer[30], and cervical cancer[31]. Today, researchers have gradually found that miR-125a-5p is also closely related to LOH. The miR-125a-5p level was reduced in the plasma of LOH patients, and this has the potential to serve as a novel biomarker in the diagnosis of LOH[12]. Accordingly, in the process of H_2O_2-induced TM3 cell apoptosis, the expression of miR-125a-5p was reduced. MiRNAs have the ability to bind to the 3′ UTR region of a target mRNA and repress gene expression by conscribing RNA-induced silencing complexes[32]. A previous study showed that miR-125a-5p could bind to the 3′ UTR region of breast cancer susceptibility gene 1-associated protein 1, thus promoting breast cancer cell apoptosis and retarding breast cancer progression[33]. In this study, NDRG2, a positive regulator for LC apoptosis[7], proved to be a direct target gene of miR-125a-5p. By suppressing NDRG2 expression, miR-125a-5p overexpression may decrease cell apoptosis and elevate the testosterone concentration in MIR22HG-overexpressed TM3 cells. To sum up, our present study further revealed the essential role of miR-125a-5p and clarified its regulation mechanism in LC apoptosis.

In conclusion, the current study elucidates that MIR22HG functions as a ceRNA to aggravate LC apoptosis in LOH by targeting the miR-125a-5p/NDRG2 axis. Our study highlights the role of MIR22HG in LOH pathogenesis, emphasizes its regulatory relationship with miR-

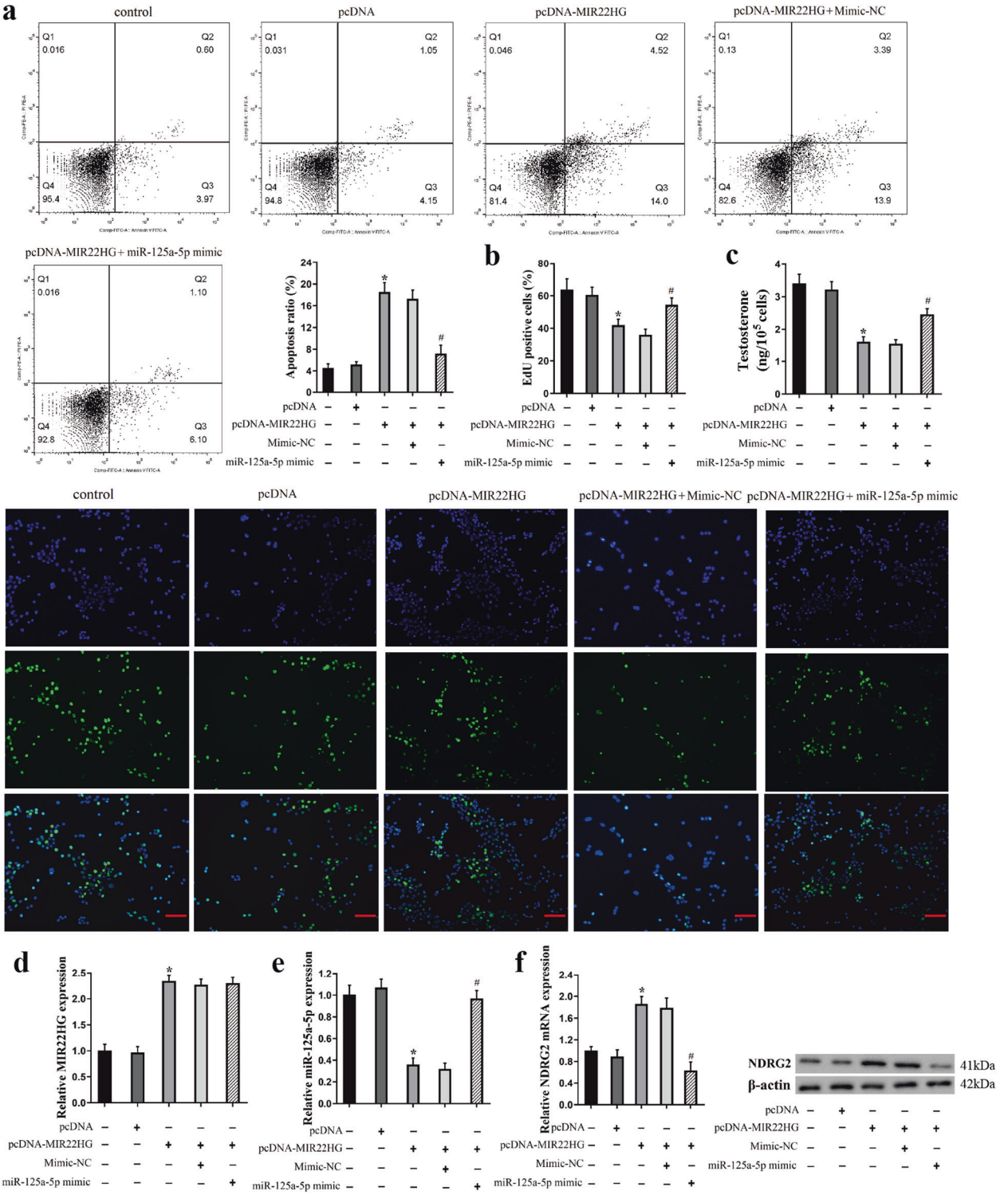

Fig. 5 Overexpression of miR-125a-5p reversed cell apoptosis and NDRG2 upregulation induced by pcDNA-MIR22HG in TM3 cells. TM3 cells were divided into five groups: control, pcDNA, pcDNA-MIR22HG, pcDNA-MIR22HG+ miR-125a-5p mimic, pcDNA-MIR22HG+ Mimic-NC, 48 h after transfection, cells were harvested. **a** The ratio of apoptotic cells was quantified using flow cytometry. **b** Cell proliferation was detected using EdU immunofluorescence analysis (Scale bar = 100 μm) and the EdU positive cells (green) were calculated. DAPI (blue) was used to counterstain the cell nucleus. **c** The concentration of testosterone in cells was determined using ELISA. The expression levels of (**d**) MIR22HG and (**e**) miR-125a-5p were determined using qRT-RCR. **f** The expression level of NDRG2 was measured by qRT-RCR and western blot. $^{*}P < 0.05$ vs. pcDNA, $^{\#}P < 0.05$ vs. pcDNA-MIR22HG+ Mimic-NC.

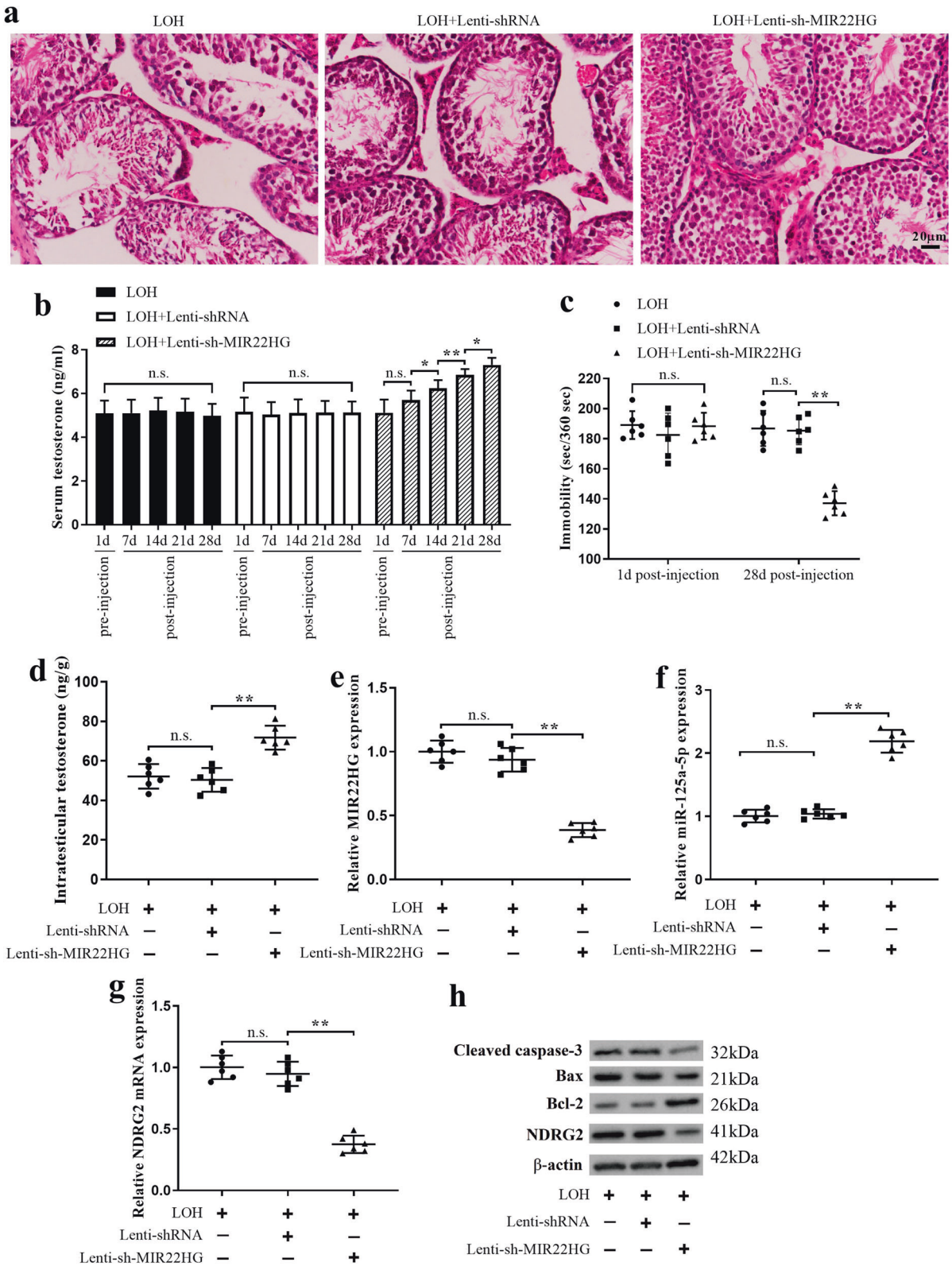

Fig. 6 MIR22HG knockdown promoted testosterone secretion in mice with LOH. Mice with LOH were divided into three groups: LOH ($n = 6$), LOH + Lentivirus vectors containing shRNA-MIR22HG (Lenti-sh-MIR22HG) ($n = 6$), LOH + the negative control of Lenti-sh-MIR22HG (Lenti-shRNA) ($n = 6$). **a** H&E staining performed on testicular tissues of mice ($n = 3$ per group and the representative images were shown, scale bar = 20 μm). **b** Serum samples of each group were collected from mice's tails 1 day before and 7, 14, 21, and 28 days after lentivector (Lenti-sh-MIR22HG or Lenti-shRNA) injection and the serum testosterone concentration was quantified using ELISA ($n = 6$). **c** Tail suspension test was performed 1 day before and 28 days after lentivector injection. **d** Intratesticular testosterone concentrations of each group were quantified using ELISA. The expression levels of (**e**) MIR22HG, (**f**) miR-125a-5p, and (**g**) NDRG2 were determined using qRT-RCR. **h** The protein abundances of cleaved caspase-3, Bax, Bcl-2, and NDRG2 were measured by western blot. *$P < 0.05$; **$P < 0.01$, n.s. no significant difference.

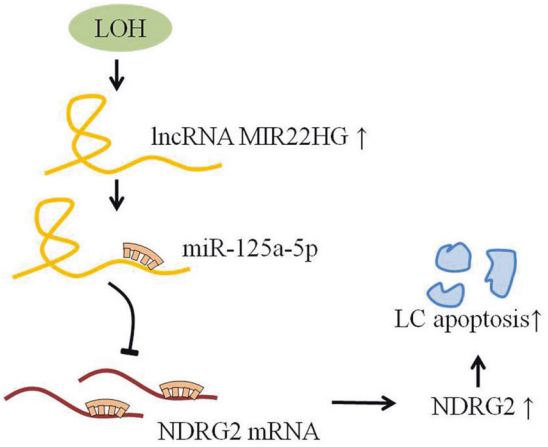

Fig. 7 MIR22HG aggravates LC apoptosis in LOH by targeting the miR-125a-5p/NDRG2 axis. MIR22HG upregulated NDRG2 expression through targeting miR-125a-5p, thus promoting LC apoptosis in LOH.

125a-5p and NDRG2, and provides a new perspective for LOH therapy.

REFERENCES

1. Shin, Y. S. & Park, J. K. The optimal indication for testosterone replacement therapy in late onset hypogonadism. *J. Clin. Med.* **8**, 209 (2019).
2. Xu, W. et al. Protective effect of calretinin on testicular Leydig cells via the inhibition of apoptosis. *Aging* **9**, 1269–1279 (2017).
3. Zhao, X. et al. Nicotine induced autophagy of Leydig cells rather than apoptosis is the major reason of the decrease of serum testosterone. *Int. J. Biochem. Cell. Biol.* **100**, 30–41 (2018).
4. Ma, Y. et al. KLF4 inhibits colorectal cancer cell proliferation dependent on NDRG2 signaling. *Oncol. Rep.* **38**, 975–984 (2017).
5. Shen, L. et al. NDRG2 facilitates colorectal cancer differentiation through the regulation of Skp2-p21/p27 axis. *Oncogene* **37**, 1759–1774 (2018).
6. Ma, Y. L. et al. N-Myc downstream-regulated gene 2 (Ndrg2) is involved in ischemia-hypoxia-induced astrocyte apoptosis: a novel target for stroke therapy. *Mol. Neurobiol.* **54**, 3286–3299 (2017).
7. Hou, W. G. et al. Differential expression of N-Myc downstream regulated gene 2 (NDRG2) in the rat testis during postnatal development. *Cell Tissue Res.* **337**, 257–267 (2009).
8. Hou, W. et al. Altered expression of NDRG2 in the testes of experimental rat model of cryptorchidism. *Urology* **75**, 985–991 (2010).
9. Li, T. et al. Up-regulation of NDRG2 through nuclear factor-kappa B is required for Leydig cell apoptosis in both human and murine infertile testes. *Biochim. Biophys. Acta* **1822**, 301–313 (2012).
10. Xu, X. et al. miR-125a-5p inhibits tumorigenesis in hepatocellular carcinoma. *Aging* **11**, 7639–7662 (2019).
11. Naidu, S. et al. PDGFR-modulated miR-23b cluster and miR-125a-5p suppress lung tumorigenesis by targeting multiple components of KRAS and NF-kB pathways. *Sci. Rep.* **7**, 15441 (2017).
12. Chen, Y.-P. et al. The plasma miR-125a, miR-361 and miR-133a are promising novel biomarkers for late-onset hypogonadism. *Sci. Rep.* **6**, 23531–23531 (2016).
13. Ghoshal-Gupta, S. et al. TIMP-1 downregulation modulates miR-125a-5p expression and triggers the apoptotic pathway. *Oncotarget* **9**, 8941–8956 (2018).
14. Song, X., Kyi-Tha-Thu, C., Takizawa, T., Naing, B. T. & Takizawa, T. 1700108J01Rik and 1700101O22Rik are mouse testis-specific long non-coding RNAs. *Histochem. Cell Biol.* **149**, 517–527 (2018).
15. Kurihara, M. et al. A testis-specific long non-coding RNA, lncRNA-Tcam1, regulates immune-related genes in mouse male germ cells. *Front. Endocrinol.* **8**, 299 (2017).
16. Zhang, D. Y. et al. Identification and functional characterization of long non-coding RNA MIR22HG as a tumor suppressor for hepatocellular carcinoma. *Theranostics* **8**, 3751–3765 (2018).
17. Salmena, L., Poliseno, L., Tay, Y., Kats, L. & Pandolfi, P. P. A ceRNA hypothesis: the Rosetta Stone of a hidden RNA language? *Cell* **146**, 353–358 (2011).
18. Duan, Z. Y. et al. U6 can be used as a housekeeping gene for urinary sediment miRNA studies of IgA nephropathy. *Sci. Rep.* **8**, 10875 (2018).
19. Wang, K. et al. The long noncoding RNA CHRF regulates cardiac hypertrophy by targeting miR-489. *Circ. Res.* **114**, 1377–1388 (2014).
20. Zang, Z.-J. et al. Effects of velvet antler polypeptide on sexual behavior and testosterone synthesis in aging male mice. *Asian J. Androl.* **18**, 613–619 (2016).
21. Jacobsen, J. P. et al. Insensitivity of NMRI mice to selective serotonin reuptake inhibitors in the tail suspension test can be reversed by co-treatment with 5-hydroxytryptophan. *Psychopharmacology* **199**, 137–150 (2008).
22. Ding, X., Wang, D., Li, L. & Ma, H. Dehydroepiandrosterone ameliorates H2O2-induced Leydig cells oxidation damage and apoptosis through inhibition of ROS production and activation of PI3K/Akt pathways. *Int. J. Biochem. Cell Biol.* **70**, 126–139 (2016).
23. Corona, G., Rastrelli, G., Maseroli, E., Forti, G. & Maggi, M. Sexual function of the ageing male. *Best Pract. Res. Clin. Endocrinol. Metab.* **27**, 581–601 (2013).
24. Weng, B. et al. Genome-wide analysis of long non-coding RNAs and their role in postnatal porcine testis development. *Genomics* **109**, 446–456 (2017).
25. Jan, S. Z. et al. Unraveling transcriptome dynamics in human spermatogenesis. *Development* **144**, 3659–3673 (2017).
26. Akhade, V. S., Dighe, S. N., Kataruka, S. & Rao, M. R. S. Mechanism of Wnt signaling induced down regulation of mrhl long non-coding RNA in mouse spermatogonial cells. *Nucleic Acids Res.* **44**, 387–401 (2016).
27. Hong, S. H. et al. Profiling of testis-specific long noncoding RNAs in mice. *BMC Genom.* **19**, 539–539 (2018).
28. Wu, Y. et al. LncRNA MIR22HG inhibits growth, migration and invasion through regulating the miR-10a-5p/NCOR2 axis in hepatocellular carcinoma cells. *Cancer Sci.* **110**, 973–984 (2019).
29. Nishida, N. et al. MicroRNA-125a-5p is an independent prognostic factor in gastric cancer and inhibits the proliferation of human gastric cancer cells in combination with trastuzumab. *Clin. Cancer Res.* **17**, 2725–2733 (2011).
30. Jiang, L. et al. Hsa-miR-125a-3p and hsa-miR-125a-5p are downregulated in non-small cell lung cancer and have inverse effects on invasion and migration of lung cancer cells. *BMC Cancer* **10**, 318 (2010).
31. Fan, Z. et al. MiR-125a suppresses tumor growth, invasion and metastasis in cervical cancer by targeting STAT3. *Oncotarget* **6**, 25266–25280 (2015).
32. Bartel, D. P. MicroRNAs: target recognition and regulatory functions. *Cell* **136**, 215–233 (2009).
33. Yan, L. et al. MiR-125a-5p functions as a tumour suppressor in breast cancer by downregulating BAP1. *J. Cell Biochem.* **119**, 8773–8783 (2018).

AUTHOR CONTRIBUTIONS

Y.L. and G.Q. conceived and designed the study and drafted the paper. F.H., P.D., and J.W. collected the data and F.G., M.S., and Y.S. contributed to the statistical analysis. Y.L. interpreted the data. G.Q. put forward the concept of the study and reviewed the paper. All authors read and approved the final paper.

FUNDING

This study was supported by the grant from the National Natural Science Foundation of China (Grant No. 81700693).

COMPETING INTERESTS

The authors declare no competing interests.

ETHICS APPROVAL AND CONSENT TO PARTICIPATE

All protocols in this study have been approved by the Ethics Committee of the First Affiliated Hospital of Zhengzhou University.

CONSENT FOR PUBLICATION

All authors consent for publication.

ADDITIONAL INFORMATION

Supplementary information The online version contains supplementary material available at https://doi.org/10.1038/s41374-021-00645-y.

Correspondence and requests for materials should be addressed to G.-j.Q.

Reprints and permission information is available at http://www.nature.com/reprints

Publisher's note Springer Nature remains neutral with regard to jurisdictional claims in published maps and institutional affiliations.